Polymer 51 (2010) 5424–5431

Contents lists available at ScienceDirect

Polymer

journal homepage: www.elsevier.com/locate/polymer

Preparation and characterization of novel ZnS/sulfur-containing polymer nanocomposite optical materials with high refractive index and high nanophase contents

Zhe Lin, Yuanrong Cheng, Hao Lü, Liang Zhang, Bai Yang*

State Key Laboratory of Supramolecular Structure and Materials, College of Chemistry, Jilin University, Changchun 130012, People's Republic of China

ARTICLE INFO

Article history:
Received 7 June 2010
Received in revised form
3 September 2010
Accepted 8 September 2010
Available online 16 September 2010

Keywords:
High refractive index
Bulk nanocomposites
Abrasion resistant

ABSTRACT

A series of novel transparent bulk ZnS-polymer nanocomposites with high refractive index were successfully prepared via in-situ bulk polymerization in the presence of 2-mercaptoethanol (ME)-capped ZnS NPs. The polymerization mechanism combined the step-growth and free radical polymerization of different monomers of episulfide, m-xylylene diisocyanante (XDI), 2-hydroxyethyl methacrylate (HEMA) and N,N-dimethylacrylamide (DMAA). The high refractive index of episulfide compounds, including ESGMES, ESDGEBA and MPS, were synthesized and used as monomers in polymerization systems. The cured nanocomposites with 30 wt% nanoparticles show high refractive index and good transparency. The refractive index of the nanocomposites could be continuously regulated in the range from 1.59 to 1.65 by the content of ZnS NPs and the pencil hardness is round about 5H. The content of ME–ZnS NPs can affect the thermal stability, mechanical and optical properties of the resulting nanocomposites, and the relationship between them were studied by TGA, DMA, pencil hardness test, Charpy impact test.

1. Introduction

Polymer-nanoparticle composites have attracted much interest owing to their excellent optical, mechanical, magnetic, electronic, and gas barrier properties. In particular, the organic–inorganic nanocomposites with high refractive index and transparency were desirable in the areas like high reflective and antireflection coatings, ophthalmic lenses, optical waveguides, filters, optical adhesives, prisms, non-linear optical materials, etc [1–9]. Several important methods have been used to synthesize high refractive index organic–inorganic nanocomposites, such as sol–gel route, in/ex-situ synthesis method [10–14]. But high refractive index organic–inorganic nanocomposites reported in the recent literatures are focused on films thinner than 10 μm. Transparent bulk nanocomposites more than 1 mm are required in several optical applications such as filters and ophthalmic lenses. However there were few reports in this field compared to nanocomposite film materials.

An effective method to improve the refractive index of hybrid optical materials is to introduce high refractive index domains (TiO_2, ZrO_2, CeO_2, PbS, ZnO, and etc.) into polymer matrix on the nanoscale [15–19]. It is clear that the hybrid material with higher nanophase content could has a higher refractive index. At present, in the studies on fabricating transparent organic–inorganic bulk nanocomposites, the content of inorganic nanofillers in polymer matrix is generally lower than 5 wt% [20–22]. Thus, in order to acquire high refractive index bulk materials, the content of inorganic particles must reach a high loading level. Because of the inherently hydrophilic character and high specific surface energies, the inorganic particles could aggregate easily in organic matrix. And the transmittance of bulk material will generally decrease with the increasing content of nanoparticles and sample thickness. Hence, it is more difficult to prepare bulk transparent optical nanocomposites with high nanophase content.

Selecting a high refractive index polymer matrix will be another effective method to synthesize high refractive index hybrid material. Most of the previous works usually employed conventional polymer matrix, such as polydimethylsiloxane (PDMS), poly(methyl methacrylate) (PMMA), polycarbonate (PC) and the refractive indices of these polymers are usually round about 1.5 [15–19]. So selecting a new polymer matrix with high refractive index is necessary. But it is hard to search a suitable one. On one hand, designing organic molecule structure to enhance material's refractive index is limited. The refractive indices of these organic materials usually round about 1.7, some could reach 1.8 till 2.7. The organic polymers with high refractive index commonly possess large birefringence and high

* Corresponding author. Tel.: +86 431 85168478; fax: +86 431 85193423.
E-mail address: byangchem@jlu.edu.cn (B. Yang).

0032-3861/$ – see front matter © 2010 Elsevier Ltd. All rights reserved.
doi:10.1016/j.polymer.2010.09.017

optical dispersion. These restrict their practical applications in optics field. On the other hand, the compatibility between the organic matrix and inorganic particles should also be considered. Thus, the development of high refractive index organic polymer matrix with excellent optical properties and good compatibility is a challenging topic. In this study, three types of episulfide-type resins were first used as organic–inorganic hybrid optical material monomers. These materials exhibited high refractive index and other several advantages such as good heat resistance, small shrinkage, chemical resistance, and excellent mechanical properties [23–25]. In addition, the ZnS nanoparticles could disperse into the episulfide-type resins by the existence of other monomers.

On the basis of these considerations, here we designed two novel types of bulk ZnS-polymer nanocomposites with high refractive index and high inorganic nanophase content. In this work, we used a simple method for the large scale production of 2-mercaptoethanol (ME)-capped ZnS nanoparticles, and then immobilized them into polymer matrix to prepare high refractive index bulk materials [26]. The ZnS NPs with a diameter of 2–5 nm exhibit a high refractive index ($n_d^{20} = 2.63$ at 620 nm) and have various applications in optical fields because of low absorption coefficient over a wide range of wavelength. Similar to halogen, the element of sulphur could improve the refractive index of polymer optical materials. In particular, the episulfides can obviously improve the refractive index of the resulting optical materials while remaining the low optical dispersity when they were used as monomers [23,24]. Episulfide-type resins also have several advantages such as good heat resistance, small shrinkage, chemical resistance, and excellent mechanical properties [25]. In this article, we synthesized three types of high refractive index episulfide compounds including 3-mercaptopylene sulfide (MPS, $n_d^{20} = 1.58$), episulfide derivative of diglycidyl ether of bisphenol A (ESDGEBA, $n_d^{20} = 1.61$) and bis(β-epithiopropylthioethyl) sulfide (ESGMES, $n_d^{20} = 1.635$). These episulfide compounds can also react with M-xylylene diisocyanante (XDI). XDI could also react with the hydroxyls on the surface of ZnS NPs. And the hydrophilic ZnS NPs were led into the hydrophobic polymerization system in this way. The monomer N,N-dimethylacrylamide (DMAA) plays an important role not only as a free radical polymerization monomer, but also as an effective dispersant and stabilizer of ME-capped ZnS NPs. 2-hydroxyethyl methacrylate (HEMA) has both hydroxyl group and carbon–carbon double bond. It was used as comonomer and crosslinker for the two types of polymerization parts. Hence, we synthesized a series of bulk ZnS-polymer nanocomposites with different monomers and complex polymerization relationship. The optical, thermal, mechanical and physical properties of the obtained nanocomposites were characterized in detail. And the relationship between composition, structures (monomer structure, polymer structure, interaction between the two phases) and properties was also discussed intensively. In particular, the obtained bulk ZnS-polymer nanocomposites exhibit higher refractive indices than the nanocomposites in the previous works when they are in the same nanophase content [26,27].

2. Experimental

2.1. Materials

Bis(β-epoxypropylthioethyl) sulfide (DGEMES) was prepared by the method referenced to the literature [28]. Bis(β-epithiopropylthioethyl) sulfide (ESGMES) was synthesized according to patent literature [29]. The episulfide derivative of diglydicyl ether of bisphenol A (ESDGEBA) was synthesized from diglycidyl ether of bisphenol A (DGEBA) as previously reported [30]. Zinc acetate dihydrate, thiourea (TU), 2-mercaptoethanol (ME), dimethylformamide (DMF), DGEBA (Guangzhou Epoxy Based Electronic Corp), N,N-dimethylacrylamide (DMAA,TCI), m-xylylene diisocyanante (XDI, Japan TCI), 2-hydroxyethyl methacrylate (HEMA), 2,3-dimercaptopropan-1-ol (DMP), potassium thiocyanate (KSCN), 2,2′-thiodiethanol (TDG, Fluka), 3-chloro-1,2-epoxypropane (ECH), acetic anhydride, tri-n-butylamine, sodium hydrogen carbonate were all of analytical-grade reagents and were used as received. 2,2′-azobisisobutyronitrile (AIBN) was recrystallized from ethanol. ME-capped ZnS NPs were prepared from $Zn(Ac)_2 \cdot 2H_2O$, TU and ME in DMF on a large scale of more than 10 g as reported previously [26].

2.2. Synthesis of 3-mercaptopylene sulfide (MPS)

MPS was synthesized from DMP in a process similar to that reported in the literature [31]. 60 g DMP was added in 120 mL of concentrated hydrochloric acid. The mixture was stirred vigorously for 48 h at room temperature, then watered down and extracted with ether. The extracts were washed and dried with anhydrous sodium sulfate, and ether was removed under reduced pressure, to give the crude chloro-dithiol. 360 mL of 10 wt% solution of sodium hydrogen carbonate was added into the crude chloro-dithiol. The mixture was stirred vigorously for 2 h at room temperature, giving off carbon dioxide. MPS was extracted into ether, washed with distilled water. Then the organic phase was dried with anhydrous sodium sulfate. After the solvents were removed, the crude MPS product was distilled under reduced pressure to obtain MPS as an almost colourless foul-smelling liquid. Yield 30%, $n_d^{20} = 1.58$; IR spectrum (cm^{-1}): 3061, 2984, 2933, 2911, 2550, 2361, 2084, 1439, 1424, 1346, 1246, 1202, 1155, 1096, 1043, 967, 945, 912, 879, 788, 716, 660, 636, 615. ^1H NMR ($CDCl_3$): (ppm) 1.71(t, 1H), 2.31 (dd, 1H), 2.61 (dd, 1H), 2.67 (m, 1H), 2.96 (dd, 1H), 3.17 (dd, 1H).

2.3. Preparation of transparent ZnS-polymer nanocomposites

2.3.1. ESGMES/ESDGEBA/XDI/HEMA/DMAA/ZnS system

The episulfide monomers ESGMES and ESDGEBA were mixed with XDI and HEMA in the desired ratio at 60 °C. The desired amount (in wt%) of ME-capped ZnS powder was dispersed into DMAA under sonication at 75 °C. After cooling, the monomer mixture of ESGMES, ESDGEBA, XDI and HEMA was dropped into ZnS/DMAA solution, and then added AIBN and tri-n-butylamine into the system. After stirring a few seconds, the transparent mixture was poured into glass-plate mold (10 cm × 6 cm × 4 mm, treated with release agent). The glass mold was degassed in a vacuum desiccator for 6 min and then put into an oven at 80 °C for 12 h, then at 90 °C, 100 °C for 2 h each and at 120 °C for 4 h. Here, the molar ratio of episulfide compounds/XDI/HEMA was selected as 1:1.2:0.2. The content of DMAA in the mixture of ESGMES, ESDGEBA, XDI, HEMA and DMAA is 30 wt%. Different content of ME–ZnS NPs are added into the polymerization system to prepare a series of nanocomposites. The amount of AIBN is 2 wt‰ of HEMA and DMAA. The amount of tri-n-butylamine is 8 wt‰ of the total system.

2.3.2. MPS/XDI/HEMA/DMAA/ZnS system

The desired amount (in wt%) of ME-capped ZnS powder was dispersed into DMAA under sonication at 75 °C. After cooling, MPS, XDI, HEMA, AIBN and tri-n-butylamine were added into the system. Then the mixture was poured into a glass-plate mold (10 cm × 6 cm × 4 mm, treated with release agent). After vacuum degassing, a step heating process (80 °C for 12 h, then at 90 °C, 100 °C for 2 h each, and at 120 °C for 4 h) was carried out. Here, the molar ratio of MPS/XDI/HEMA was selected as 1:1.2:0.2. The content of DMAA in the mixture of MPS, XDI, HEMA and DMAA is 30 wt%. Different content of ME–ZnS NPs are added into the polymerization system to prepare a series of nanocomposites. The

amount of AIBN is 2 wt‰ of HEMA and DMAA. The amount of tri-n-butylamine is 8 wt‰ of the total system.

2.4. Characterization

FTIR spectra were recorded using a Nicolet AVATAR 360 FTIR spectrophotometer. Transmission electron microscopy (TEM) was carried out using a Hitachi H-8100 transmission electron microscope. UV–vis spectra of the bulk nanocomposites were characterized on a Shimadzu UV 3100. The X-ray powder diffraction (XRD) patterns of ME–ZnS NPs and nanocomposite materials were taken on a Siemens D-5005 X-ray diffractometer with Cu Kα ($\lambda = 1.5418$ Å) radiation. Surface hardness was examined using an ASTM D3633. The refractive index of bulk nanocomposite was measured by W2S-1 refractometer at 20 °C. The thermogravimetric analysis (TGA) was performed on a Netzsch STA 449C thermogravimetric analyzer. A TA Q800 device was used for the dynamic thermomechanical behavior study by the 3-point bending method. The total luminous transmittance and haze of materials were recorded by a WGW photoelectric hazemeter. Charpy impact tests were obtained with a Charpy pendulum impact tester.

3. Results and discussion

3.1. Structure of bulk nanocomposite materials

Several different types of monomers were used in this work to form transparent, high refractive index polymer matrix. The structural formulas of the monomers are summarized in Fig. 1. Three types of episulfide were selected to improve the refractive index of the materials. The isocyanate groups of XDI can react with both episulfide monomers by ring-opening copolymerization and hydroxyl groups on the ZnS NPs by polyaddition reaction. Consequently ZnS NPs were immobilized covalently into polymer matrix stably. It was found that DMF can stabilize ZnS NPs by coordinating to the surface of the nanoparticles [32]. The monomer DMAA with a carbon–carbon double bond has a structure approximate to DMF. Thus DMAA plays an important role not only as a free radical polymerization monomer but also an effective dispersant and stabilizer of ME-capped ZnS NPs. HEMA has hydroxyl group and carbon–carbon double bond, so it could react with both XDI and DMAA. Consequently, HEMA was used as comonomer and crosslinker for the two types of polymerization parts. Thus the introduction of HEMA could prevent phase separation. Attributed to the complex polymeric relation, the inorganic particles were distributed into polymer matrix uniformly and the two different polymer parts were cross-linked without phase separation. Fig. 1 provides the possible structures formed in the resulting bulk materials with and without ZnS NPs based on the complex polymerization systems.

3.2. Cured ESGMES/ESDGEBA/XDI/HEMA/DMAA/ZnS resins

It can be seen in Fig. 3 that the episulfide monomer of ESDGEBA is an aromatic group-containing compound, and ESGMES is a long-chain aliphatic compound. Thus the copolymerization of ESDGEBA with ESGMES can improve the mechanical properties and heat resistance of the optical materials [25]. And the structure of the nanocomposite is described in Fig. 2 in detail.

The molar ratio of episulfide compounds/XDI/HEMA was fixed at 1:1.2:0.2. However, the molar ratio of ESGMES and ESDGEBA could be changed, which could affect the properties of the cured resin. ESGMES has higher refractive index than ESDGEBA. ESDGEBA has higher pencil hardness and lower density. If the molar ratio of ESGMES and ESDGEBA could reach an appropriate value, the nanocomposite will has both high refractive index and high pencil hardness. Thus we prepared a series of samples with different molar ratios of ESGMES and ESDGEBA. The weight ratio of ME–ZnS NPs was fixed at 10 wt%. The properties of the nanocomposites are summarized in Table 1. Compared with other molar contents of ESGMES in episulfide compounds, the sample with 70 mol% of ESGMES has the highest refractive index and better transparency.

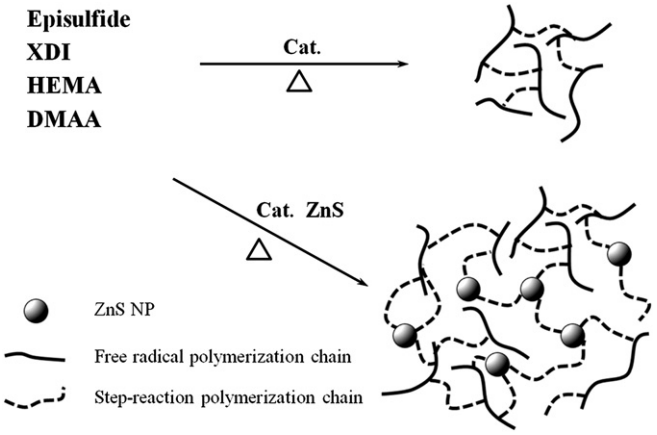

Fig. 1. Structures of (A) pure polymer and (B) nanocomposite with ZnS NPs.

We fixed the molar content of ESGMES in episulfide monomers at 70%, and prepared a series of bulk nanocomposites with different ME–ZnS NPs contents. The properties of these nanocomposites are summarized in Table 2. Fig. 4 shows the FTIR spectra of pure ME–ZnS NPs and the nanocomposites with different ZnS NPs contents. The absorption peak of the S–H vibration at 2550–2565 cm^{-1} is not observed in the IR spectrum, indicating that the mercapto groups of ME were coordinated to the ZnS NPs surface [32]. The characteristic peaks of episulfide groups at 610 cm^{-1} and isocyanate groups at 2270 cm^{-1} disappeared in the polymer. The peak at 3347 cm^{-1} for N–H stretching vibration appeared after polymerization. With the increasing content of ZnS NPs, the peak at 2071 cm^{-1} becomes more and more apparent [33]. At the same time, the content of ME increased. Thus the peaks for $-CH_2-$ group at 2917 cm^{-1} and for O–H band at 3421 cm^{-1} gave much intense absorbance than polymer matrix. There were three different kinds of C=O bonds in the nanocomposite: The peak at 1695 cm^{-1} was caused by the absorption of C=O bond in –NH–CO–S–; The peak at 1722 cm^{-1} was for C=O stretching vibration in PHEMA. When we put ME–ZnS NPs into polymer matrix, the XDI reacted with the hydroxyl groups on the surface of nanoparticles to form the –NH–CO–O–, the peak of the C=O bond in –NH–CO–O– was at 1644 cm^{-1}. With the increase the ZnS NPs content, the peak intensity of C=O bond at 1644 cm^{-1} in FTIR spectra enhances. As the consumption of XDI, the content of the C=O bond in –NH–CO–S– decreased, so the peak at 1695 cm^{-1} became inconspicuous, while the peak at 1722 cm^{-1} for C=O stretching vibration in PHEMA became visible. Thus C=O stretching band region shows different patterns.

The XRD patterns of ZnS NPs and the nanocomposites with different ZnS NPs contents are shown in Fig. 5. The peaks at 2θ values of 28.5°, 47.5° and 56.3° corresponding to (111), (220) and (311) planes show that the ZnS NPs have the cubic structure of sphalerite. The resulting ZnS crystallite structure is in accordance with that reported previously [32c,34]. And the ZnS NPs in the nanocomposite retains its cubic crystal structure. With increasing ZnS NPs content, the intensities of diffraction peaks increase gradually. It indicates that the ZnS NPs have been incorporated into the bulk polymer matrices successfully. TEM images of the nanocomposites with different ZnS contents of 5 wt%, 15 wt% and 25 wt%

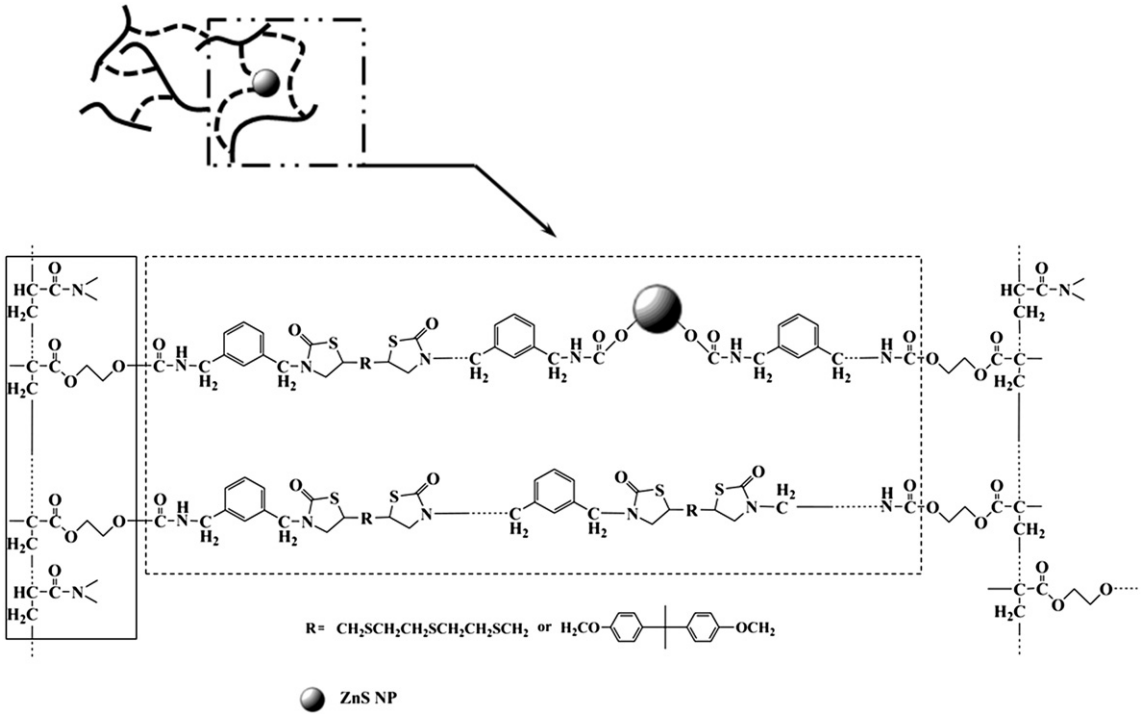

Fig. 2. Structure of the nanocomposite obtained from ESGMES/ESDGEBA/XDI/HEMA/DMAA system.

are presented in Fig. 6. It can be seen that the diameter of ZnS NPs is about 2–4 nm and dispersed uniformly in the polymer matrices. According to Rayleigh's law, such small particles will not cause apparent light scattering, thus the bulk nanocomposites should have good visible light transmittance. Just like it is shown in UV–vis transmittance spectra.

Fig. 7A displays the UV–vis transmittance spectra of the ESGMES/ESDGEBA/XDI/HEMA/DMAA/ZnS bulk nanocomposites with different ZnS NPs content (approximate thickness: 4 mm). It can be seen that the nanocomposites exhibit good transparency in the visible light range even when the ZnS NPs content is as high as 20%. The transmittance decreases with increasing content of ZnS NPs because of the partial aggregation of nanoparticles and macroscopic phase separation. Fig. 7B shows a photograph of the bulk nanocomposites with 30 wt% ME–ZnS NPs. The total luminous transmittance and haze of the nanocomposites were tested by a WGW photoelectric hazemeter and the results are listed in Table 2. The obtained bulk nanocomposites possess the total luminous transmittance greater than 74% and the haze lower than 9%.

The TGA curves of ME–ZnS NPs and nanocomposites with different ZnS NPs contents are shown in Fig. 8. Because of the unstable ME capping agent, the ME–ZnS NPs begin to decompose at about 199 °C, while the polymer without nanoparticles exhibits a higher initial decomposition temperature of 236.8 °C. The nanocomposites show a conspicuous weight loss between 250 and 300 °C, which is similar to ME–ZnS NPs. However, the resulting nanocomposites have a similar thermal stability property as the polymer matrix. It also can be found that the content of pure ZnS in the capped particles is about 50 wt% and many capped organic molecules are present on the ZnS NPs surface. With increasing ZnS NPs content, the residues of the bulk nanocomposites increase. And the residues of samples measured by TGA are in good accordance with that of the calculated values of pure ZnS in the nanocomposites.

The dynamic mechanical analysis (DMA) was used to characterize the nanocomposite samples (see Fig. 9A). We can see that when we introduce ZnS NPs into reaction system, the storage modulus of nanocomposite is higher than the polymer matrix. In our system, the two long-chain episulfide monomers were used. The rigidity of polymer matrix is lower than the ZnS NPs'. When the ZnS NPs content increase, the homodisperse ZnS NPs capped by the short chain of ME react with XDI and play a role as framework of the nanocomposite, hence the rigidity of the whole nanocomposite increase. With the increase of the test temperature, the storage modulus of nanocomposite descends quickly. Fig. 9B presents the damping factor (tan δ) versus temperature curves for bulk

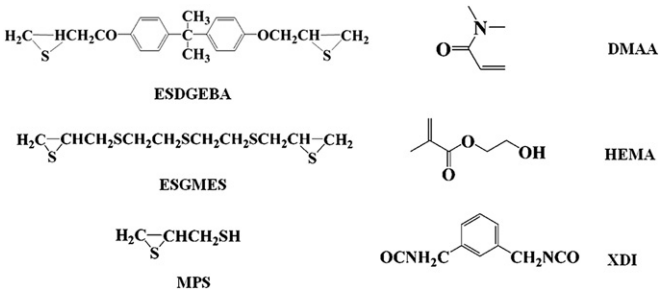

Fig. 3. Structures of episulfide monomers, diisocyanante and other monomers.

Table 1
Properties of ZnS-polymer bulk nanocomposites with different ESGMES contents.

ESGMES[a] (mol%)	n_d[b]	ρ[c] (g/cm^{-3})	Pencil Hardness	T%[d]
0	1.5968	1.2839	5H	75.6
30	1.6020	1.2914	4H	71.4
50	1.6035	1.2998	4H	80.8
70	1.6072	1.2974	3H	79.6
100	1.6125	1.3131	3H	74.5

[a] Theoretical molar content of ESGMES in episulfide monomers.
[b] Refractive index.
[c] Density of nanocomposites.
[d] Total luminous transmittance (%).

Table 2
Properties of ESGMES/ESDGEBA/XDI/HEMA/DMAA/ZnS composites with different ZnS NPs contents.

ZnS[a] (wt%)	n_d[b]	Density[c] (g/cm^3)	Pencil Hardness	IPS[d] (kJ/m^2)	T_g[e] (°C)	T_d[f] (°C)	Residue[g] (wt%)	T[h] (%)	Haze[i] (%)	US[j] (nm)
0	1.5911	1.2513	1H	1.05	71.1	236.8	9.33	81.7	5.0	346
5	1.6000	1.2753	2H	1.21	86.2	231.4	11.95	80.5	5.9	348
10	1.6072	1.2974	3H	2.35	80.7	228.8	13.94	79.6	6.5	341
15	1.6134	1.3248	4H	3.47	76.8	214.2	16.80	78.3	7.1	337
20	1.6275	1.3566	4H	4.51	73.4	211.6	19.79	75.4	7.9	332
25	1.6316	1.3880	4H	1.98	71.0	212.6	20.98	75.2	8.5	329
30	1.6410	1.4122	5H	1.06	68.3	210.1	23.21	74.5	8.9	326

[a] Theoretical weight content of ME-capped ZnS NPs in the nanocomposite materials.
[b] Refractive index.
[c] Density of nanocomposites.
[d] Impact strength.
[e] Glass transition temperature (T_g) obtained from DMA results.
[f] Thermal decomposition temperature.
[g] Char yield of the nanocomposites at 850 °C based on the experimental results from TGA.
[h] Total luminous transmittance (%).
[i] Haze tested by WGW photoelectric hazemeter.
[j] US: the onset wavelength of total absorption.

nanocomposites with different ZnS NPs contents. The peak values in tan δ curves of ZnS-polymer materials are higher than that the polymer matrix's. It is because the ZnS NPs make the degree of crosslinking increase, thus the glass transition temperature (T_g) grows up. However, T_gs of the nanocomposites decrease when the ZnS NPs content is above 15 wt% due to the plasticizing effect of ME–ZnS NPs. The introduction of ZnS NPs changes the intrinsic physical crossling points of polymer networks. The abundance of ZnS NPs with surface capping organic agents in the nanocomposite plays a role of plasticizer. In addition, the nanocomposites have only one T_g, this indicates that the monomers are polymerized into the homogeneous phase materials, although there are two polymerization mechanism (free radical and step-growth polymerization) in our system. So the nanocomposites still exhibit good transparency in the visible light range.

Pencil hardness test results are listed in Table 2. The pencil hardness of the ZnS-polymer nanocomposites could be continuously regulated in the range from 1H to 5H by the content of ZnS NPs. It can be seen that ZnS NPs have improved the hardness of the materials. Because of the structure of cross-linked macromolecules, the pencil hardness in this work is much higher than that in pioneering works with the same type of nanoparticle and nanophase content [27]. It shows that the addition of ZnS NPs can improve the impact strength to some extent, and when the content of ZnS NPs reaches 25 wt%, the impact strength starts to decrease. ZnS NPs have small grain size and large specific surface area. And they have great contact area with polymer matrix. When there is external force acting on the nanocomposite, the rigid ZnS NPs could arouse crazes and absorb impact force, thus the impact strength of material increase. But when the ZnS NPs content reaches 25 wt%, the excess ZnS NPs could cause an increase of brittleness of the nanocomposite materials. On the one hand, the distance between nanoparticles in polymer matrix is so close; crazes could combine into big cracks. On the other hand, the problem of particle dispersion arises along with the increase of nanoparticles, and stress concentration could take place. Under the external force action, the particles conglobation would slip, thus the impact strength of the material decreases.

The refractive indices of bulk nanocomposites with different ZnS NPs contents have been measured by a W2S-1 refractometer at 20 °C and the results listed in Table 2. Fig. 10 shows the relationship between the refractive index and the weight percentage of ME–ZnS NPs in bulk nanocomposites. The refractive index of the polymer matrix is 1.5911. The refractive index of the nanocomposite increases with increasing ZnS NPs content. When the ME–ZnS NPs content is 30 wt%, the refractive index of the obtained bulk nanocomposite can reach 1.6410. In the pioneering work of Lü et al., the refractive index of the obtained bulk nanocomposite with 30 wt% nanophase content was 1.59 and the refractive index could reach 1.63 when 50 wt% ZnS NPs were introduced into the polymer [26].

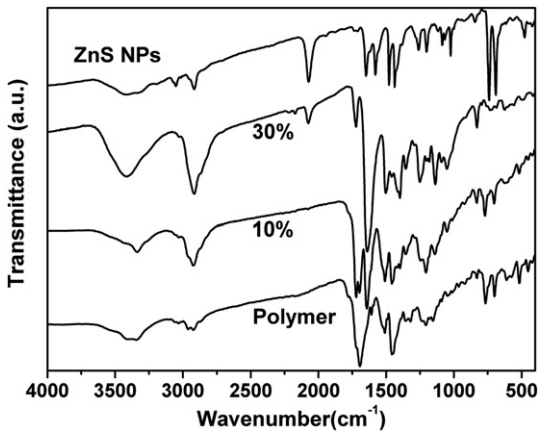

Fig. 4. FTIR spectra of ME–ZnS NPs, ESGMES/ESDGEBA/XDI/HEMA/DMAA/ZnS bulk nanocomposites with ZnS NPs contents of 0, 10 wt% and 30 wt% (molar ratio of ESGMES in episulfide monomers is 70%).

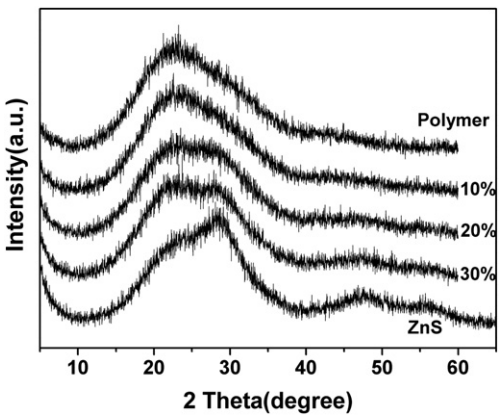

Fig. 5. XRD patterns of ME–ZnS NPs, ESGMES/ESDGEBA/XDI/HEMA/DMAA/ZnS bulk nanocomposites with ZnS NPs contents of 0, 10 wt%, 20 wt% and 30 wt% (molar ratio of ESGMES in episulfide monomers is 70%).

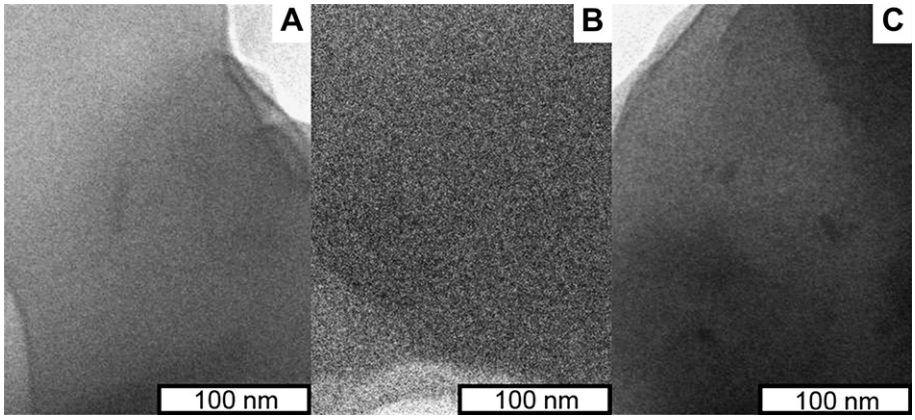

Fig. 6. TEM images of the nanocomposites with ZnS NPs contents of (A) 5 wt%, (B) 15 wt% and (C) 25 wt% respectively.

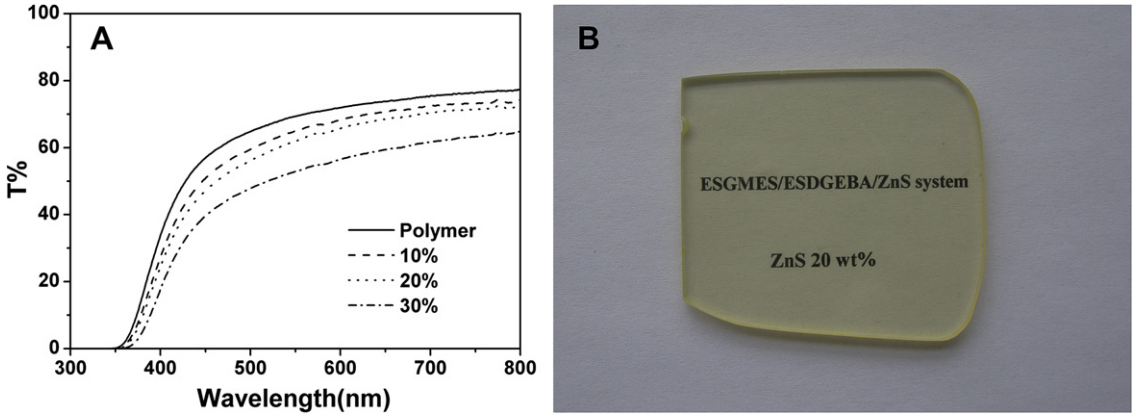

Fig. 7. (A) UV–vis transmittance spectra of the ESGMES/ESDGEBA/XDI/HEMA/DMAA/ZnS bulk nanocomposites with ZnS NPs contents of 0, 10 wt%, 20 wt% and 30 wt% (molar ratio of ESGMES in episulfide monomers is 70%); (B) Photograph of the ESGMES/ESDGEBA/XDI/HEMA/DMAA/ZnS bulk nanocomposites with 20 wt% ZnS NPs (sample thickness: 4 mm).

In the work of Cheng et al., the refractive index of the obtained bulk nanocomposite with 30 wt% nanophase content was 1.58 [27]. Comparing with these works, the nanocomposites obtained in our work could exhibit higher refractive indices in much lesser nanophase contents. This indicates that the introduction of episulfide as monomer to improve the refractive index of nanocomposite is very efficacious. The refractive index of ME–ZnS NPs is calculated to be about 1.790 by regression analysis of the trace in Fig. 10. The value is lower than that of bulk ZnS ($n_{ZnS} = 2.368$) because of the existence of ME ($n_{ME} = 1.4996$) molecules on the ZnS NPs surface.

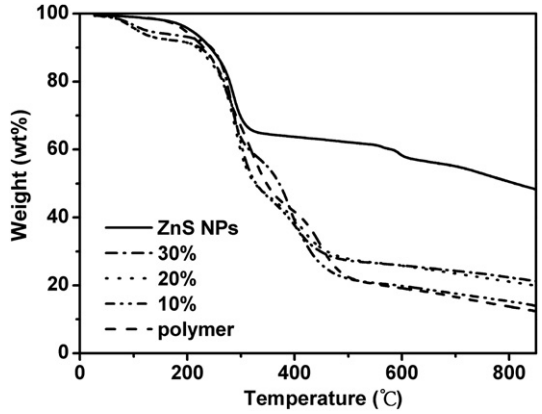

Fig. 8. TGA curves of ME–ZnS NPs and the ESGMES/ESDGEBA/XDI/HEMA/DMAA/ZnS bulk nanocomposites with ZnS NPs contents of 0, 10 wt%, 20 wt% and 30 wt% (molar ratio of ESGMES in episulfide monomers is 70%).

3.3. Cured MPS/XDI/HEMA/DMAA/ZnS resins

It shows in Fig. 1 that the episulfide monomer of MPS is a short-chain aliphatic compound, and the refractive index of MPS is 1.58. Thus MPS can improve the refractive index of the polymer matrix. MPS is liquid at room temperature and ESGMES and ESDGEBA are solids. So MPS was easier to prepare nanocomposite compared with ESGMES and ESDGEBA in the technical aspect. Furthermore MPS has both cyclic sulfide group and thiol group, so it has higher reactive activity than ESGMES and ESDGEBA. And the structure illustration of the polymer matrix is described in Fig. S1 in detail.

The properties of the cured MPS/XDI/HEMA/DMAA/ZnS resins with different ZnS contents are listed in Table 3. The UV–vis transmittance spectra of the MPS/XDI/HEMA/DMAA/ZnS bulk nanocomposites (approximate thickness: 4 mm) with different ZnS NPs contents and a photograph of the bulk nanocomposite with 20 wt% ZnS content are shown in Fig. S2A. It can be seen that the nanocomposites exhibit good transparency in the visible light range even when the ZnS NPs content is as high as 30 wt%. The total luminous transmittance and haze of the nanocomposites were tested by a WGW photoelectric hazemeter and the results are listed in Table 3. The obtained bulk nanocomposites possess high total luminous transmittance (>76%) and low haze (<5.9%).

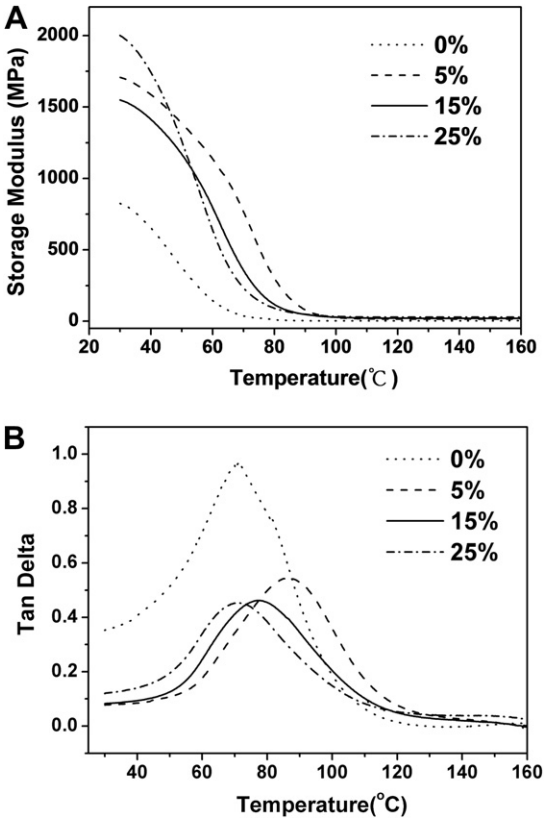

Fig. 9. Dynamic mechanical analysis (DMA) of the ESGMES/ESDGEBA/XDI/HEMA/DMAA/ZnS bulk nanocomposites with ZnS NPs contents of 0, 5 wt%, 15 wt% and 25 wt% (molar ratio of ESGMES in episulfide monomers is 70%). (A) Storage modulus versus temperature curves for nanocomposites with different ZnS contents; (B) Damping factor (tanδ) versus temperature curves for nanocomposites with different ZnS contents.

The DMA curves of nanocomposites samples are present in Fig. S3. In the Fig. S3A, we can see that when the content of ZnS NPs is 25 wt%, the storage modulus of the nanocomposite is lower than the pure polymer. And in Fig. S3B, the peak values of nanocomposites in tan δ curves are lower than that in the polymer matrix's tan δ curves. These phenomena are different from that showed in ESGMES/ESDGEBA/ZnS system. The result may be the difference of the episulfide monomers' structures.

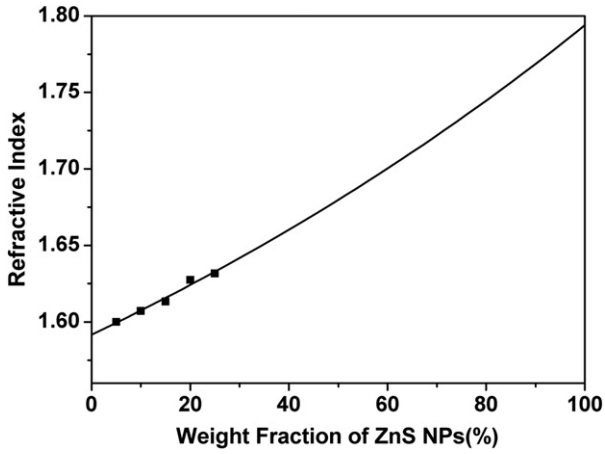

Fig. 10. Refractive indices of ESGMES/ESDGEBA/XDI/HEMA/DMAA/ZnS bulk nanocomposites at different weight fractions of ME–ZnS NPs (molar ratio of ESGMES in episulfide monomers is 70%).

MPS is a short-chain episulfide monomer with both cyclic sulfide group and thiol group. It has higher reactive activity than ESGMES and ESDGEBA. When we introduced the ZnS NPs into monomers mixture, the reaction of the system was so quick that the ZnS NPs couldn't react with XDI in time. So a majority of the ZnS NPs could not enter into the cross-linked network by covalent link. Thus it caused by plasticizing effect of ME–ZnS NPs, the storage modulus of nanocomposite with high ZnS NPs content is lower than pure polymer. And T_gs of the nanocomposites decrease with the ZnS NPs content increase for the same reason. In addition, like the ESGMES/ESDGEBA/ZnS system the nanocomposites also have only one T_g, this demonstrated that the monomers are polymerized into a homogeneous material.

Pencil hardness test and the Charpy impact results are listed in Table 3. The pencil hardness of the ZnS-polymer nanocomposites could be continuously regulated in the range from 4H to 6H by the content of ZnS NPs. It also can be seen that ZnS NPs could improve the hardness of the nanocomposites. The increase of ZnS NPs affects a change of the state of impact strength. The variation trend and mechanism are the same as that in the ESGMES/ESDGEBA/ZnS system.

It also can be seen in Table 3 that the refractive index of the polymer matrix in this system is 1.5953. The refractive index of the nanocomposite increases with increasing ZnS NPs content. The

Table 3
Properties of MPS/XDI/HEMA/DMAA/ZnS composites with different ZnS NPs contents.

ZnS[a] (wt%)	n_d[b]	Density[c] (g/cm^3)	Pencil Hardness	IPS[d] (kJ/m^2)	T_g[e] (oC)	T_d[f] (°C)	Residue[g] (wt%)	T[h] (%)	Haze[i] (%)	US[j] (nm)
0	1.5953	1.2823	4H	0.67	86.6	232.8	4.45	89.8	4.0	323
5	1.6063	1.2915	4H	1.01	81.7	223.5	9.02	83.9	4.1	355
10	1.6121	1.3004	4H	1.78	80.5	222.1	9.36	82.7	4.5	333
15	1.6201	1.3222	5H	2.15	78.3	219.5	14.56	81.8	4.8	325
20	1.6347	1.3484	5H	3.54	76.2	216.2	15.94	80.8	5.0	329
25	1.6390	1.3655	5H	4.06	74.1	212.7	22.90	79.9	5.2	335
30	1.6475	1.3821	6H	2.16	71.1	208.9	26.71	76.4	5.9	340

[a] Theoretical weight content of ME-capped ZnS NPs in the nanocomposite materials.
[b] Refractive index.
[c] Density of nanocomposites.
[d] Impact strength.
[e] Glass transition temperature (T_g) obtained from DMA results.
[f] Thermal decomposition temperature.
[g] Char yield of the nanocomposites at 850 °C based on the experimental results from TGA.
[h] Total luminous transmittance (%).
[i] Haze tested by WGW photoelectric hazemeter.
[j] US: the onset wavelength of total absorption.

refractive index is 1.6475 when the ZnS NPs content reaches 30 wt %. This type of ZnS-polymer nanocomposite has a little higher refractive index than the cured ESGMES/ESDGEBA/XDI/HEMA/DMAA/ZnS resins with the same nanophase content. The refractive index of ME–ZnS NPs is also lower than that of bulk ZnS ($n_{ZnS} = 2.368$) because of the existence of ME ($n_{ME} = 1.4996$) molecules on the ZnS NPs surface.

4. Conclusions

In summary, we have developed a simple and effective method for the preparation of transparent bulk nanocomposites with high refractive index ($n_d = 1.64$). The nanocomposites were easily prepared by curing episulfide, XDI, HEMA with the mixture of DMAA and ME–ZnS NPs. The experimental results showed that the bulk ZnS-polymer obtained from the episulfide compounds presented good optical, thermal, mechanical properties, etc. It indicated that the introduction of episulfide monomers and ME–ZnS NPs was effective for improving refractive index of the nanocomposites. The refractive index of the ZnS-polymer nanocomposites could be continuously regulated in the range from 1.59 to 1.65 by the content of ZnS NPs. And the refractive index could reach 1.64 with 30 wt% nanophase content. In particular, the nanocomposites obtained in our work exhibit higher refractive indices with much lesser nanophase contents than that in the pioneering works. In addition, the introduction of ME–ZnS NPs into the copolymerization system can improve surface hardness and crosslinking degree of the system simultaneously. The ZnS-polymer nanocomposite has a highest pencil hardness round about 5H–6H. The bulk nanocomposites with well-balanced properties have potential application in fabricating optical materials with tunable refractive indices and high abrasion resistance.

Acknowledgments

The authors appreciate the financial support of the National Natural Science Foundation of China (No. 20921003 and 50973039) and the Program of Technological Progress of Jilin Province (20090620).

Appendix. Supplementary material

Supplementary data associated with this article can be found, in the online version, at doi:10.1016/j.polymer.2010.09.017.

References

[1] Okutsu R, Ando S, Ueda M. Chem Mater 2008;20:4017.
[2] Cui ZC, Lü CL, Yang B, Shen JC, Su XP, Yang H. Polymer 2001;42:10095.
[3] Nebioglu A, Leon JA, Khudyakov IV. Ind Eng Chem Res 2008;47:2155.
[4] Dobrowolski JA, Ho F. Appl Opt 1982;21:288.
[5] Hart SD, Maskaly GR, Temelkuran B, Prideaux PH, Joannopoulos JD, Fink Y. Science 2002;296:510.
[6] Yablonovitch E. Science 2000;289:557.
[7] Kitai AH. Solid state luminescence. London: Chapman & Hall; 1993.
[8] Hornak LA, editor. Polymers for lightwave, integrated optics: technology, applications. Dekker Marcel; 1992.
[9] Klimov VI, Mikhailovsky S, Xu S, Malko S, Hollingsworth JA, Leatherdale CA, et al. Science 2000;290:314.
[10] Mammeri F, Bourhis EL, Rozes L, Sanchez C. J Mater Chem 2005;15:3787.
[11] Pénard A-L, Gacoin T, Boilot J-P. Acc Chem Res 2007;40:895.
[12] Kypriandou T-L, Caseri W, Suter UW. J Phys Chem 1994;98:8992.
[13] Nakayamaa N, Hayashi T. J Appl Polymer Sci 2007;105:3662.
[14] Zhou S, Wu L. Macromol Chem Phys 2008;209:1170.
[15] Nussbaumer R, Caseri W, Smith P, Tervoort T. Macromol Mater Eng 2003;288:44.
[16] Lee S, Shin H-J, Yoon S-M, Yi D, Choi J-Y, Paik U. J Mater Chem 2008;18:1751.
[17] Lü CL, Guan C, Liu YF, Cheng YR, Yang B. Chem Mater 2005;17:2448.
[18] Althues H, Henle J, Kaskel S. Chem Soc Rev 2007;36:1454.
[19] Yang Y, Li YQ, Fu SY, Xiao HM. J Phys Chem C 2008;112:10553.
[20] Demir MM, Memesa M, Castignolles P, Wegner G. Macromol Rapid Commun 2006;27:763.
[21] Gao M, Yang Y, Yang B, Bian F, Shen JC. J Chem Soc Chem Commun 1994:2779.
[22] Pavel FM, Mackay RA. Langmuir 2000;16:8568.
[23] Kayanoki Hisayuki, Ishizuka Satoshi, Takigawa Akio. Eur Pat 0524477, 1993.
[24] Tamura Yutaka, Watari Fumie. Eur Pat 0424144, 1991.
[25] Lü CL, Cui ZC, Wang Y, Yang B, Shen JC. J Appl Polym Sci 2003;89:2426.
[26] Lü CL, Cheng YR, Liu YF, Liu F, Yang B. Adv Mater 2006;18:1188.
[27] Cheng YR, Lü CL, Lin Z, Liu YF, Guan C, Lü H, et al. J Mater Chem 2008;18:4062.
[28] Lü CL, Cui ZC, Zhao D, Yang B. Chem J Chin Univ 2001;22:1924.
[29] Akikazu A, Motoharu T, Kenichi T. Eur Pat 761665, 1997.
[30] Charlesworth JM. J Polym Sci Polym Phys Ed 1979;17:329.
[31] Doyle FP, Holland DO, Mansford KRL, Nayler JHC, Queen A. J Chem Soc; 1960:2660.
[32] (a) Hosokawa H, Murakoshi K, Wada Y, Yanagida S, Satoh M. Langmuir 1996;12:3598;
(b) Hosokawa H, Fujiwara H, Murakoshi K, Wada Y, Yanagida S, Satoh M. J Phys Chem 1996;100:6649;
(c) Murakoshi K, Hosokawa H, Tanaka N, Saito M, Wada Y, Sakata T, et al. Chem Commun; 1998:321;
(d) Wankhede ME, Haram SK. Chem Mater 2003;15:1296.
[33] Strommen DP, Plane RA. J Chem Phys 1974;60:2643.
[34] Lü CL, Cui ZC, Li Z, Yang B, Shen JC. J Mater Chem 2003;13:526.